Evaluation of turbulence models and mesh types for CFD simulation of air distribution in a mechanical ventilated pig house containing animal models

Hao Li, Li Rong, Guoqiang Zhang*

Department of Engineering, Aarhus University, Blichers Allé 20, P. O. Box 50, 8830 Tjele, Denmark

* Corresponding author. Email: Guoqiang.Zhang@eng.au.dk

Abstract

There is increasing tendency to use Computational Fluid Dynamics (CFD) method in study of flow distributions in farm animal buildings. Turbulence models are generally considered to be important on the results due to the approximations of the turbulence in varied scales. Although some studies have been conducted on the evaluation of turbulence model in simulation of airflow in ventilated rooms, knowledge of the airflow in animal occupant zone considering animal blocking and thermal convection effects is still limited. In this study, five commonly used two equation turbulence models (standard k-ε, realizable k-ε, RNG k-ε, standard k-ω, and SST k-ω) were applied to model the airflow motion in a mechanically ventilated pig room with animal models in pens. In addition, non-conformal mesh which combines several sub computational domains and connecting the boundary of domains by interface was tested. The effect of mesh ratio on the interface was studied based on fully structural hexahedral mesh (SH). Investigation is conducted by application of unstructured tetrahedral mesh (UT) in the animal occupied zone (AOZ) and SH in the rest room domain. The results showed that turbulence model had not strong effect on the main airflow pattern except the RNG k-ε model. The tested ratios of resolution on interfaces were found not strongly impacting the predicted airflow distributions. The usage of UT in the AOZ sub domain also provided acceptable results. It is concluded that the non-conformal mesh is an alternative for animal buildings with complex geometry to maintain the affordable grid numbers and reduce the difficulties in generating the mesh.

Keywords: Numerical simulation, RANS, mesh interface, pig model, pig room.

1. Introduction

It has been noticed that flow fields in pig house are crucial for creating a thermally comfortable and healthy environment for animals. Therefore, to improve the indoor environment of animal house, the air distribution should be carefully studied.

In the study of ventilation system, CFD has shown strong superiority in comparison with conventional experimental method. One of the main advantages is that it allows full control on the influencing factors and provides universal data in the computational domain with relatively low cost of time and expense. There is increasing tendency to use Computational Fluid Dynamics (CFD) method in study of flow distributions in farm animal buildings (Bartzanas et al., 2002; Bjerg et al., 2002; Rong et al., 2016; Wu et al., 2012). To better model the livestock building, animal models in real geometry have been used in some of CFD studies for environment parameters inside animal buildings (Bjerg et al., 2008; Gebremedhin and Wu, 2005; Seo et al., 2012).

Turbulence models are generally considered to be important on the results due to the approximations of the turbulence in varied scales (Rong et al., 2016; Sorensen and Nielsen, 2003). Although some studies have been conducted on the evaluation of turbulence model in simulation of airflow in ventilated rooms (Norton et al., 2010; Rong et al., 2016; Shen et al., 2012; Zhang et al., 2007), knowledge of the airflow affected by animal blocking and thermal convection is still limited. Among the turbulence modelling, generally there are RANS method and LES method, and RANS method are popular used in the scopes of agricultural research due to the sufficient high quality and low request of computational power. Therefore, five commonly used two equation turbulence models (standard k-ε, realizable k-ε, RNG k-ε, standard k- ω, and SST k- ω) based on RANS method were evaluated on a ventilated pig room containing animal models in this study.

Grid scheme is another critical factor on the simulation results. In general, it is the hexahedral, tetrahedral, and hybrid meshes are the commonly applied mesh type in the animal building simulation. The hexahedral mesh, as the first type of mesh adopted in the CFD study, is commonly considered to have more accurate results compared to tetrahedral mesh (Duan et al., 2015; Hefny and Ooka, 2009). However, the hexahedral mesh can mainly adopt on the geometry with smooth boundary, and for the complex geometry, like animal, it is almost impossible to mesh use hexahedral grids. Tetrahedral mesh, however, is capable for the boundary with complex surface. In addition, it is equipped in most of the grids generation code, and can be generated automatically. But it is known that the prediction accuracy of the tetrahedral mesh may be lower than hexahedral mesh, and the cells number can be larger than hexahedral mesh at same cell sizes, which means the computation time can be longer. For instance, the slatted floor inside the animal buildings usually has relatively small slot dimensions comparing to the building dimensions. It can make a huge cell number of mesh when fully applying tetrahedral mesh in whole room domain. Conformal hybrid mesh as a combination of hexahedral and tetrahedral mesh adopts the advantages from the two kinds of mesh, and it has been applied in the air distributions in

animal house (Seo et al., 2012). But this kind of hybrid mesh is hard to generate, especially for the case which include the grids with high aspect ratios.

Non-conformal mesh, which connecting adjacent domain boundary by interface, is used when geometry is complex. It can serve as an alternative way to mesh the complex geometry in agricultural buildings. For instance, tetrahedral mesh can be used in the animal occupied zone (AOZ) where geometry is complex and hexahedral mesh in the rest room domain. When both hexahedral mesh and tetrahedral mesh are adopted in different domain, it can be regarded as kind of hybrid mesh but without request the fully agreement of nodes on the interface boundary. Therefore, it is relatively easy to be generated compared to the aforementioned hybrid mesh. Since the nodes are not fully agreed on the boundary, the iteration data need reallocation on the boundary, the ratio of resolution on interface boundary can have impacts on the data transfer process.

On the basis of state-of-the-art CFD simulations of air distribution in pig house, this investigation was conducted for a systematic evaluation of turbulence model and mesh type. The objectives were: (1) to identify a suitable turbulence model for air speed distribution in the mechanic ventilated pig house containing heated pig model; (2) to test the impact from the ratio of resolution on the interface boundary on the air speed distribution; (3) to compare the hexahedral mesh and tetrahedral mesh modelled in the AOZ on the prediction accuracy of air speed distribution when non-conformal mesh is used.

2. Materials and Methods

2.1. Experiment setup

One pig room of the experimental pig house in climate lab in AU Foulum, with dimensions of 5.70 × 4.88 × 2.67 m^3 (L × W × H), was arranged for this experiment. The dimensions and layout of the room followed a section of typical commercial Danish pig production unit. The room was equally divided into two pens (4.8 × 2.44 m^2, L × W) by a 0.8 m high partition wall. Each pen had two thirds fully slatted floor and one third drain floor. There was a drinking trough on the side wall, and one shared feeder on the partition wall in each pen. In front of pens, there was a 0.9 m wide inspection alley. Underneath the floor, a 0.7 m deep manure pit was built for each pen. There were four artificial animals placed inside the room, in each pen two of the artificial animals were placed in the middle of the slatted floor and drained floor. The artificial animals were made of iron in a hollow cylindrical shape. Four 100W incandescent bulbs were installed inside each of the artificial animals to generate the heat. The experimental measurements were conducted under non-isothermal conditions with ventilation rate of 2533 $m^3\ h^{-1}$ operated in negative pressure and two bottom hinged flap wall inlets. Before each measurement, the ventilation system was on for around 3 h to reach steady state condition in the room. During the experiments, the ventilation rate was measured by a free running propeller and recorded by a climate control system (Vengsys, Denmark) each minute. Using omnidirectional Air Velocity Transducer (TSI, model 8475) and CR 1000 data logger (Campbell Scientific Ltd), the air speed was measured every 0.2 s and averaged every 1.0 s for a measurement period of 60 min at each measuring points. The measurement was conducted on four vertical lines in the center of the pig pen 2 (Figure 1), only the air velocity above the floor was measured, since the air velocity below floor was considered to be very low, besides, it is not the target area where this study is focusing. The room temperature and humidity were continuously measured by the sensors equipped in the room and recorded each minute by the climate control system (Vengsys, Denmark). The surface temperature of wall and artificial pigs were measured by T type thermocouples with data logger (Eltek Ltd, England) every 5min during the whole experimental process.

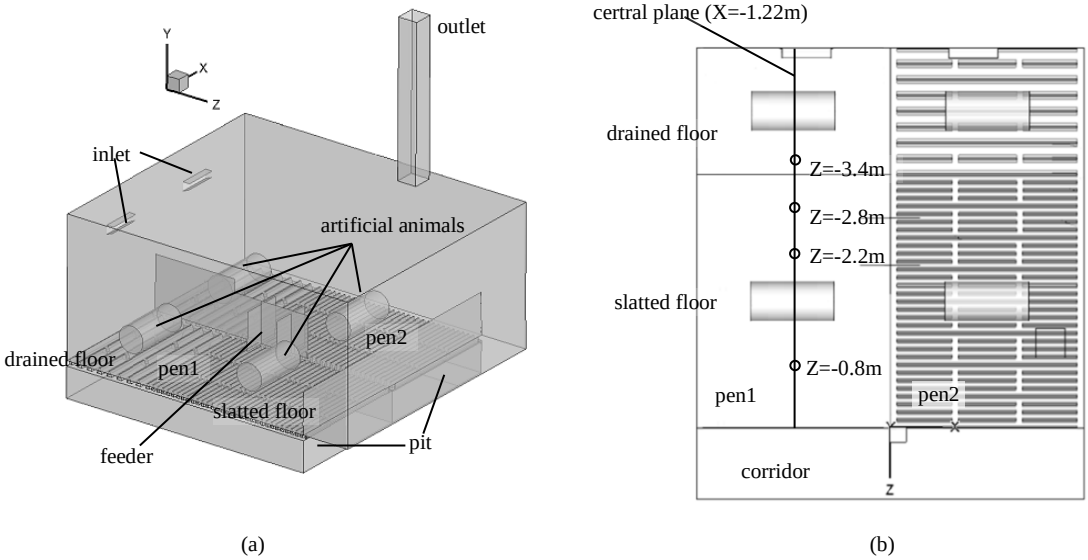

(a) (b)

Figure 1 The sketch of the geometry (a) and the measurement points for the air

2.2. CFD modelling

2.2.1. Calculation domain and grids

All the studies were based on a same geometry which was derived from the pig house in which the field measurement was conducted. In order to reduce the complexity of modelling in CFD, proper approximations were made in the study, the light and drink system were not included in the CFD modelling, and the feeders were modelled as cuboid. Since the study has two main objectives, to test the turbulence models and mesh resolution and type, the treatment of calculation domain and mesh generation were different in these two parts.

In the study of the impact of turbulence models, the calculation domain was regarded as a whole, and structural mesh was adopted for the grids. To reduce the impact from the mesh and ensure the quality of simulation, a grid independence test was conducted first. The slots on the slatted floor increased the complexity for the mesh. There were 168 slots of 10mm in width on the floor and the mesh size at the slots therefore cannot be larger than 10 mm. The cylindrical animal models on another aspect also increased the complexity of mesh, and the skewness could be higher when the cell size around the animal models was large. Therefore, low Reynold number modelling approach was used to mesh the grids around the pig models to provide a better mesh quality around the animal models and consequently a better simulation result on the airflow around animals. With all these considerations, the coarsest mesh in the grids independent test had 3.25 million cells. For the mesh in medium and dense levels, the cell numbers were 4.25 million and 6.10 million, respectively. Although the mesh can be made denser than the mesh we used in this study, for the engineering use in agriculture it is the sufficient enough.

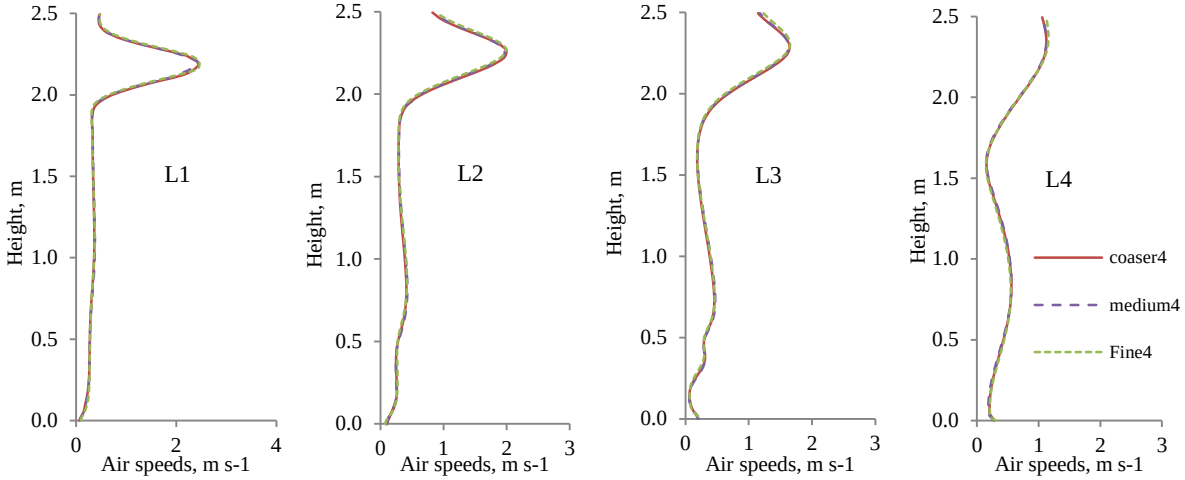

Figure 2 Grid independence test for calculation velocity profiles on the four vertical lines

Figure 2 showed the velocity profiles in four vertical measured lines in different mesh resolutions using standard k-ε model. No significant difference was found among the three resolutions on the testing heights above floor. The mesh in medium level was used for further study in evaluating the turbulence models. The coarse mesh was not selected since the slots only contain one cell on width dimension of the slots, which was consider very coarse to generate accuracy data beneath floor, although the velocity under floor was not measured and discussed in this study.

In the study of the impact of mesh interface resolution and type, the entire computational domain was divided into three parts (Figure 3), up AOZ domain, AOZ domain, and down AOZ domain. The grids in these three subdomains were generated separately. The two adjacent domains were connected by interfaces named as interface up and interface down. These three calculation domains were meshed with different grids resolutions and different mesh types were compared on the AOZ domain. The detailed information of cells numbers and mesh types are showed in Table 1.

Table 1 Combination of the three parts of computational domain in different cases

	The test of interface resolution			The test of mesh type
	Case 1	Case 2	Case 3	Case 4
Up AOZ domain	Hexahedral	Hexahedral	Hexahedral	Hexahedral
Mesh type/cells number	1850k	1233k	377k	377k
AOZ domain	Hexahedral	Hexahedral	Hexahedral	Tetrahedral
Mesh type/cells number	1534k	1534k	1534k	1397k
Down AOZ domain	Hexahedral	Hexahedral	Hexahedral	Hexahedral
Mesh type/cells number	868k	868k	868k	868k
Ratio of mesh resolution on interface up	1:1	1:1.5	1:5	1:2.3
Ratio of mesh resolution on interface down	1:1	1:1	1:1	1:1.4

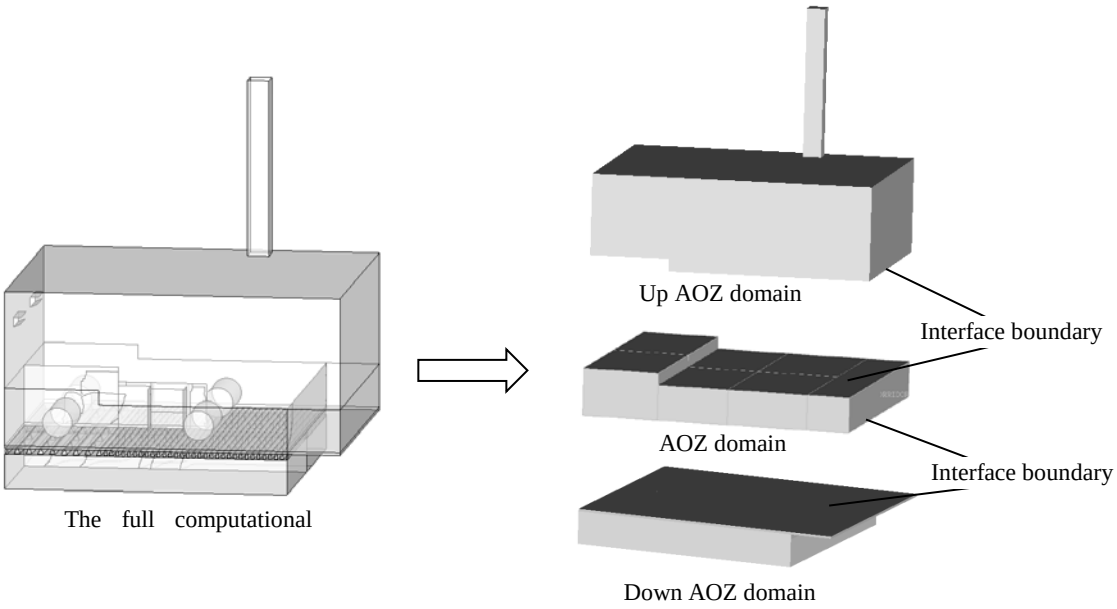

Figure 3 The divisions of the computational domain

2.2.2. Turbulence models

Turbulence models are generally considered to be important on the results due to the approximations of the turbulence in varied scales. To determine the most suitable turbulence model for use in the study, five two-equation RANS turbulence models were compared to the measurements. The turbulence models used in the evaluation included the standard k–ε model, the realizable k–ε model, the RNG k-ε model, the standard k–ω model, and the SST k-ω model. These two-equation RANS turbulence models were chosen because they were very popular ones and have widely used in both research and engineering. The standard k-ε model uses k which represents the turbulence kinetic energy to account for energy transport, and ε as dissipation rate to represents the turbulence diffusion(Launder and Spalding, 1974). The realizable k- ε model is improved based on standard k- ε on the dissipation of turbulent kinetic energy, the coefficient, C_μ, which in standard k- ε is constant, is expressed as a function of mean flow and turbulence properties (Shih et al., 1995). For the RNG k- ε model, additional terms and modifications of constants are included in the transport equations compared to standard k- ε model (Yakhot and Orszag, 1986). The standard k- ω model is based on model transport equations for the turbulence kinetic energy (k) and the specific dissipation rate (ω), and this model improved the accuracy of the model for predicting free shear flows. It improves the results for boundary layers under adverse pressure gradients compared to k- ε models(Wilcox, 1988). However, this model is sensitive to free stream, which decrease the robust of this model for the simulation in far field. The standard k-ω model used in Fluent (Ansys Inc.) is reported to have improved the accuracy of the model for predicting free shear flows by adding production terms to both the k and ω equations(Anonymous, 2013b). SST k-ω model combined the advantages of stand k-ω model in simulating the near-wall region and the robust of k- ε model in simulating the freestream in the far field(Menter, 1994). The k-ω models require fine mesh in the near-wall regions. However, in practice, a very fine mesh on all the surfaces is a challenge for mesh generation and requires a very large computational capacity. Therefore, to simplify the difficulty in mesh generation and to reduce the grids number, the low reynold modelling approach was only adopted on the region where artificial animals located. Fine mesh was generated on the surface of the artificial animals, Y plus on the surface was around 1 providing better results on the airflow near animal.

2.2.3. Data transfer between interfaces

Interface boundary is generally used to calculate the flux across the non-conformal boundary in which the hanging nodes may exist on the boundary. In this study, the interface boundary connected calculation domains were all considered as fluid zones, and an interior zone was generated on the interface where the mesh on the two domains overlapped and allowed the fluxes transfer across the domain boundaries.

The fluxes data across the interface are transferred based on the interface zone faces on the intersection (Anonymous, 2013a). Figure 4 shows an example on the data treatment on the interface. When data is transfer from domain 1 to domain 2, firstly, data on interface boundary AB are distributed into ab and bc in the new generated interface zone, while the data on boundary BC allocate into cd and de in the interface zone. Then the data on the interface zone transfer to the corresponding cells directly, for instance, It is bc and cd bring the data to cell IV from cell I and II, but not EF. Since the data are reallocated on the interface, the accuracy of the simulation may depend on the mesh ratio on the interface between two adjacent domains.

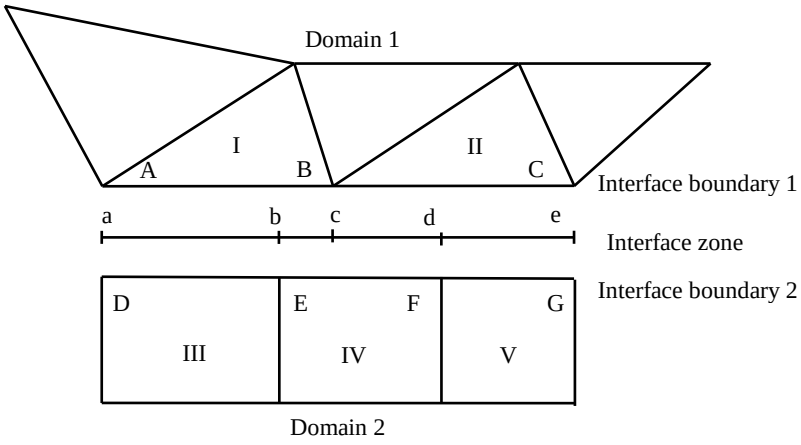

Figure 4 Example on the data transfer on the interface boundary

2.2.4. Boundary condition and numerical methods

To represent the experimental pig room as it is physically, proper boundary conditions are necessary. The wall inlet in the physical model was imposed as pressure inlet. And the outlet of the ventilated room was regarded as mass flow inlet with outwards flow to ensure the control of the ventilation rate. All the surfaces of wall, floor and pig model were imposed as non-slip wall with no roughness, since enhanced wall treatment was activated to solve the flow on the surface boundary. The temperatures of the inlet air and on the wall surface were averaged from the measurement. The boundary conditions were summarized in Table 2.

Table 2 Boundary conditions

Inlet	Pressure inlet (0 Pa), temperature of 19.8 ^{o}C.
Outlet	Mass flow inlet with revised flow in 0.862kg s^{-1} (equal to 2533 m^3h^{-1}).
Walls and floor	Non-slip wall, with the wall boundary on an average temperature of 20.8^{o}C and floor in 19.7^{o}C.
Pig model	The two pigs closing to inlet, surface temperature of 36.2 ^{o}C; The two pigs closing to the working corridor, surface temperature of 33.3 ^{o}C.

Based on the commercial CFD software Fluent 15.0 (Ansys Inc.), the simulation uses the finite volume differencing scheme in Steady Reynolds-averaged Navier–Stokes (RANS) method and SIMPLE (Semi-Implicit Method for Pressure-Linked Equations) numerical algorithm. Second-order upwind schemes were used for both the convection terms and the viscous terms of the governing equations. The criteria of convergence is set such that the residuals for u, v, w, k, ε less than 10^{-3}, and the residual for energy less than 10^{-6}. Besides, the net flow rate of the geometry, which was monitored as a supplementary convergence criterion, should be less than 10^{-4}.

3. Results

3.1. Effect of turbulence model on the results

Figure 5 shows various distributions of experimental and numerically predicted velocity magnitude on the four vertical measurement lines in pen 2. Generally, good agreements between experimental and numerical values were found for most of the turbulence models in this test, except RNG k-ε model, which had higher deviation than others although the tendency was similar with other models and experimental results. Standard k-ω model and SST k-ω model provided slightly better results than Standard k-ε model and Realizable k-ε model on the lower height. The contours of the velocity magnitude on the middle plane in the tested pen are showed in Figure 6. Similar like the velocity profile, RNG k-ε model generated a different airflow pattern compared to rest of the turbulence models which had a similar flow pattern above floor.

Generally, it can be concluded that most of the CFD models could provide a reasonable description of the airflow pattern inside this pig house. Using the experimental data as evaluation reference, it is evident that RNG k-ε model did not perform well on this specific ventilation configuration. It is different with some publications which are suggesting RNG k-ε model have high performances in different ventilation conditions (Huawei et al., 2007; Liu et al., 2013). But the conclusion is agree with the results of Rong et al. (2016) in a study conducted in a similar condition. The discrepancy on the performances of turbulence models may come from the influence of geometry and ventilation configuration. It indicated that the performance of turbulence models on prediction airflow is case depended. In this study, although the result of the k-ω models showed slightly better than the k-ε models, the deviations were not significant and the results from the k- ε models were acceptable. The geometry of this case was complex, and the robust of the turbulence model is

necessary for the iterations to reach convergence. Since the k-ε which is the most widely used in engineering and is considered to be very robust, it was chosen for the study on the impacts from interface resolutions and mesh types.

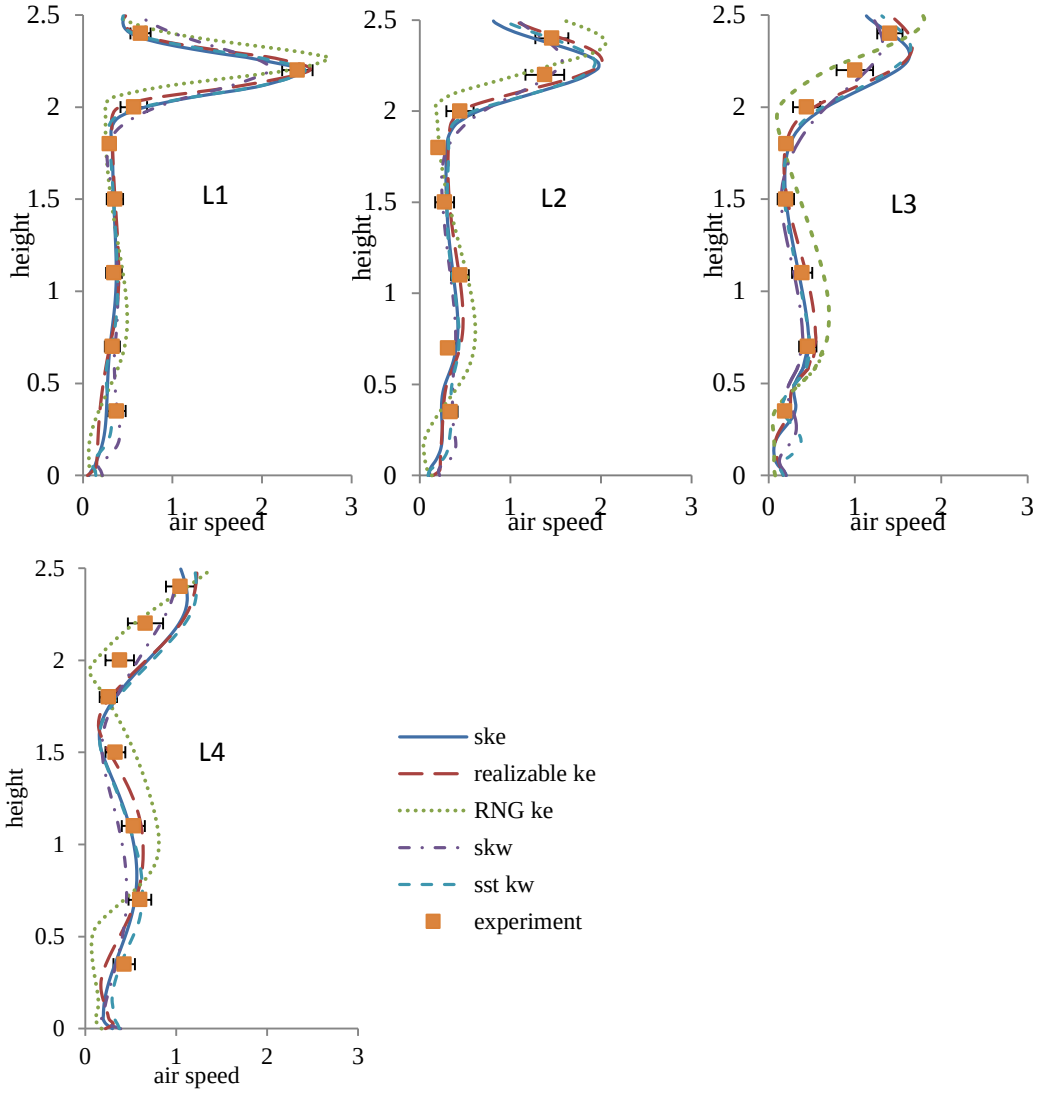

Figure 5 Air speed profile of the four vertical lines by simulation using varied turbulence model and measurement in non-isothermal condition

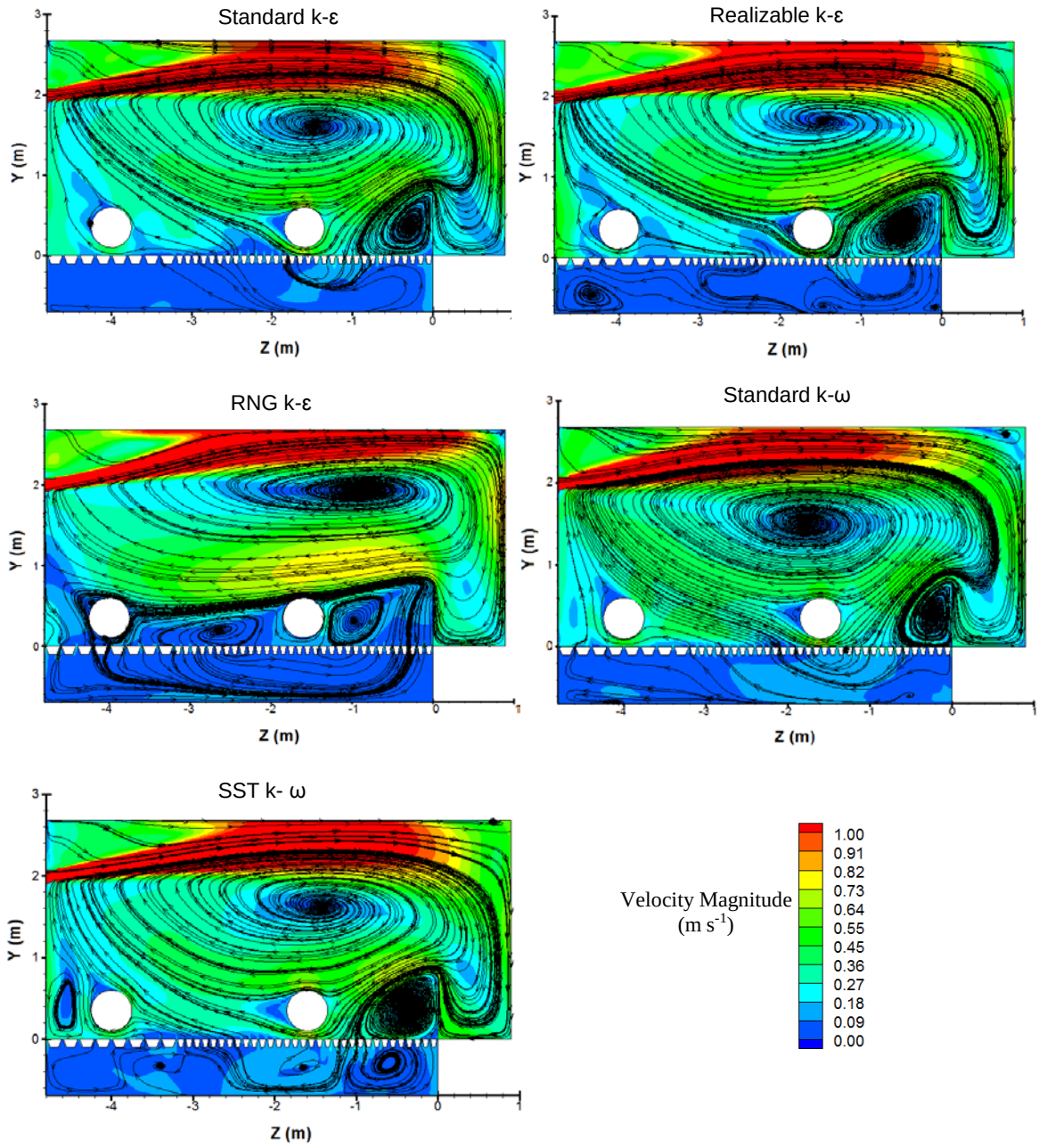

Figure 6 Contours of the velocity magnitude on the middle plane in pen 2 based on different turbulence model

3.2. Impact from the resolution of interface

Figure 7 shows various distributions of experimental and numerically predicted velocity magnitude along the symmetrical plane in the pen 2 when the resolution of the interface is different. The data in each domain were transferred continuously. All these three cases tested in the study were found sharing the same tendency with the experimental results on the four measured vertical lines. The differences between these three were relatively small. The prediction of velocity magnitude on the vertical plane in the center of pen 2 (Figure 8) showed the information was transferred through the interface smoothly. And comparing the contours between the cases with varied ratio of interface resolutions, the difference was not significant above the floor.

It is the interface zone where the fluxes data across the interface are transferred, and the data is reallocated on the boundary. Therefore, the resolution on the interface boundary should have impact on the data transfer, since the detailed information can be lost in the process of data redistribution when the ratio of the interface boundary is too high. It is always preferable if the ratio on the two adjacent interface boundaries is close to 1. When the ratio on the interface is higher than 1, and the simulation can still be validated by experimental data. The usage of interface, on the other hand, provides possibility to mesh the calculation domains in a same geometry with varied resolution. For instance, the place where detailed information is needed can be meshed in denser mesh, while the rest be meshed in a coarse mesh, and connected each other by interface. It is also a solution to reduce the iteration time since the total cells number is reduced

when interface is adopted. In this study, the iterations were conducted using 4 nodes paralleled calculation on a PC with i7-4770 CPU and 16GB memory, the iteration times for the three cases were 38.3h, 30.5h, and 22.1h, respectively, with the ratios on the interface boundary increased. It is notable that interface should better not be used where the sudden flow transition happens, since the data may be affected by the interface during the data transfer.

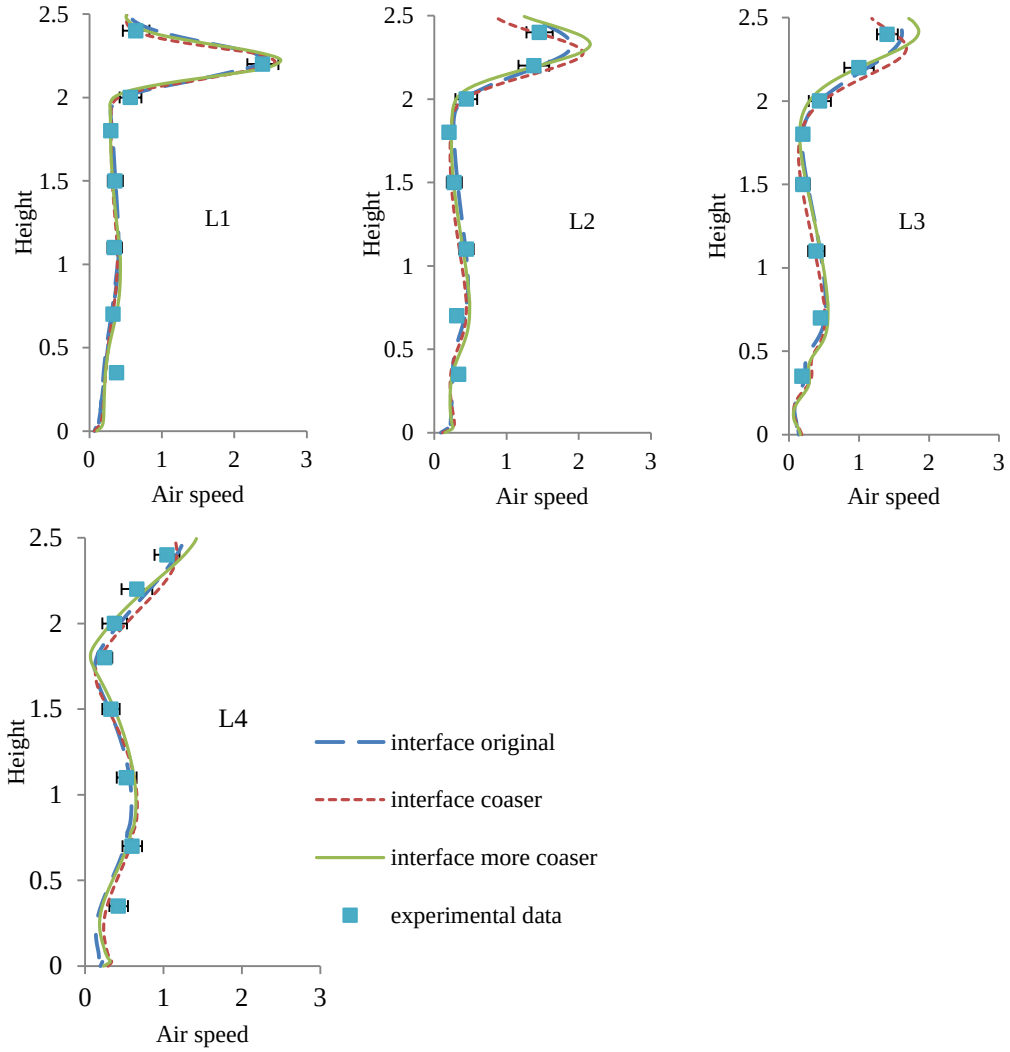

Figure 7 Air speed profiles of the four vertical lines by simulation using varied interface resolution ratios and measurement

3.3. Impact from the mesh type in AOZ

Figure 9 compares the measured airflow distributions with simulated the at a cross section in .The structured mesh in the comparison was the one which the ratio on the interfaces were both 1:1, and the second mesh type consisted both unstructured mesh (on the AOZ domain) and structured mesh (up AOZ domain and down AOZ domain) with the ratio on the interfaces 1:2.3 and 1:1.4, respectively. The difference of these two different mesh types on predicting the airflow profile in the four tested vertical lines was not significant, and both of them showed good agreement with the measured results. In figure 8, the velocity magnitude contours of the center plane in pen 2 is showed. Compared with other cases using interface, the airflow pattern was found to be similar.

It has been reported that hexahedral meshes can provide higher accuracy in predicting the airflow distribution (Duan et al., 2015; Hefny and Ooka, 2009). However, no significant out performance was observed in this study. A possible reason can be the resolution of the AOZ domain was high which provide a higher accuracy in the prediction. The unstructured tetrahedral mesh was widely used when the geometry of model is very complex, and normally it generates more cells than hexahedral mesh based on same geometry. The hybrid mesh contain both hexahedral mesh and tetrahedral mesh and connecting them by interface combined the advantage of both hexahedral and tetrahedral mesh and reduce the difficulty in modelling the complex geometry in agricultural research, like the cases which contain slatted floor or animal models.

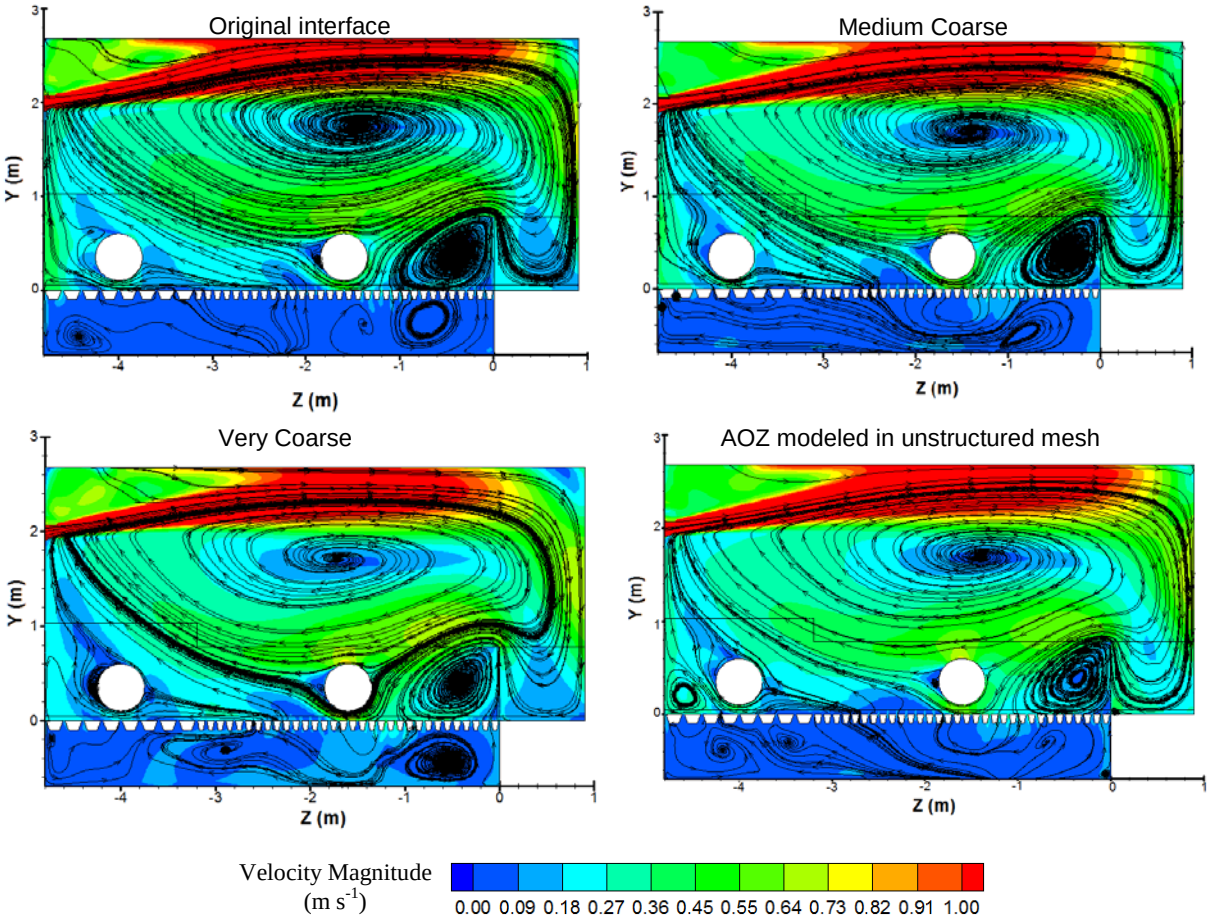

Figure 8 Contours of the velocity magnitude on the middle plane in pen 2 using interfaces

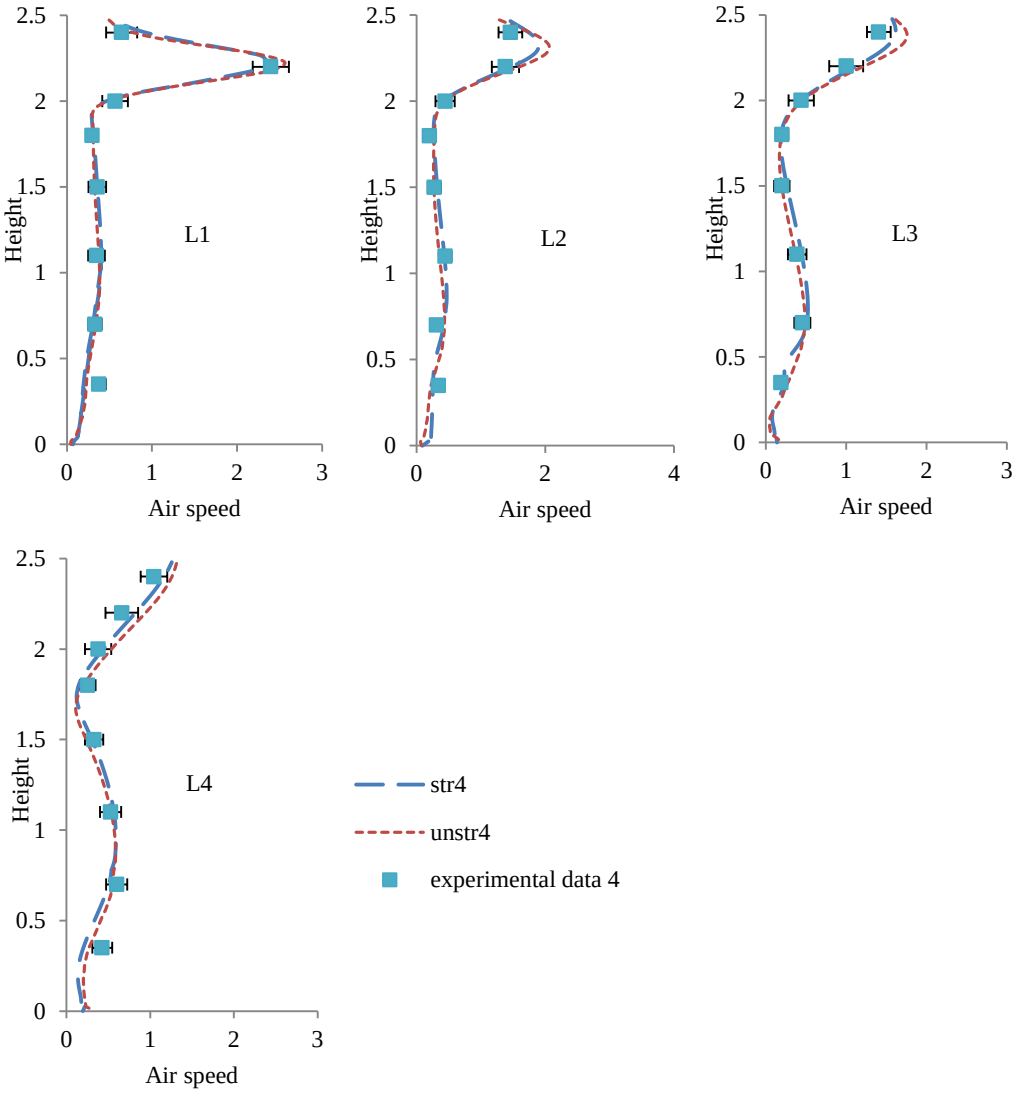

Figure 9 Comparison of air speed profiles of the four vertical lines modelled by structured and unstructured mesh

4. Case study using pig model inside

4.1. Model geometry and mesh

The case was based on the same building in the above study, and the geometry was separated into three domains as well (Figure 10). Unlike the model in the above parts, the simple cylindrical models in the AOZ domain were replaced with pig models in the similar shape of pig. 16 pigs in 50kg weight were modelled in each pen. The weight was controlled by surface area of model based on the relationship Brody et al. (1928). The distribution of the pigs referred the literatures. Unstructured tetrahedral mesh was used to generate the grids in the AOZ domain, since it is almost impossible to apply structured hexahedral mesh here in such complex geometry.

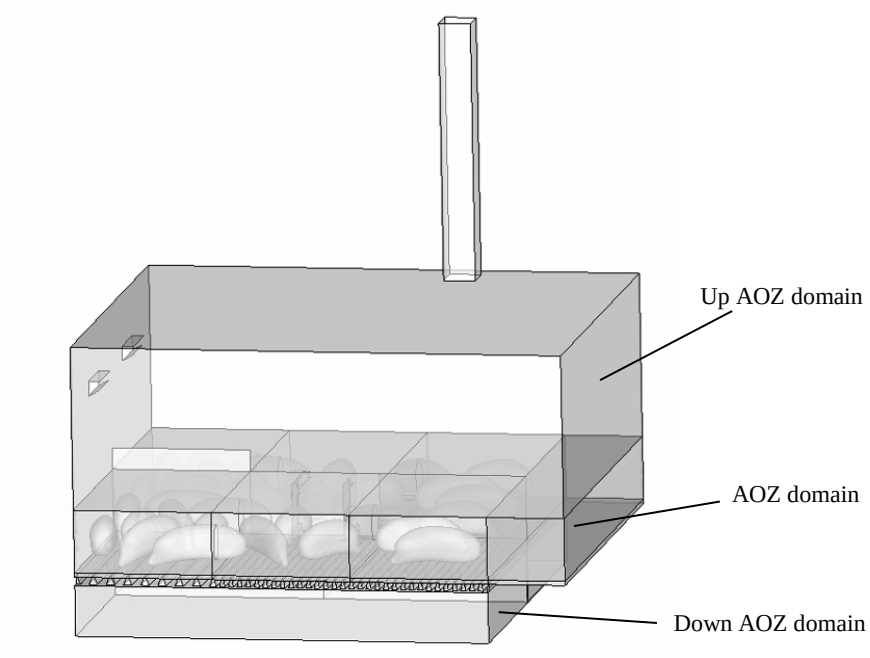

Figure 10 Geometry and the division of the computational domain

4.2. Boundary condition and numerical method

Generally, the boundary conditions were similar with aforementioned cases. The changes mainly happened on the specific values, since this case was in a virtual condition without experimental data. The ventilation rate was imposed as $3200 m^3 h^{-1}$. Since the ventilation rate was relatively strong, the heat transfer between the indoor air and wall surface and floor surface was assumed very small in a steady condition, and therefore, the surfaces of floor and wall were treated as adiabatic. For the temperature of pig surface, the core temperature of 39^oC was selected as boundary condition.

For the numerical method in this part, the calculation was calculated using the same numerical treatment as mentioned in section 2.2.3.

4.3. Results

The contour of velocity magnitude in the symmetry plan in pen 2 is illustrated in Figure 11. Like the cases studied above, there was a big vortex above the AOZ, since the mechanic ventilation on the inlet was dominating the airflow. The jet from the inlet provided the energy for the movement of the air inside the pig room. In the AOZ level, the airflow speed was found to be very low. The occupation of the pig models blocked the air movement. It indicates that the airflow passing through the back of pig can be the main force for the convective term for the heat loss from pig.

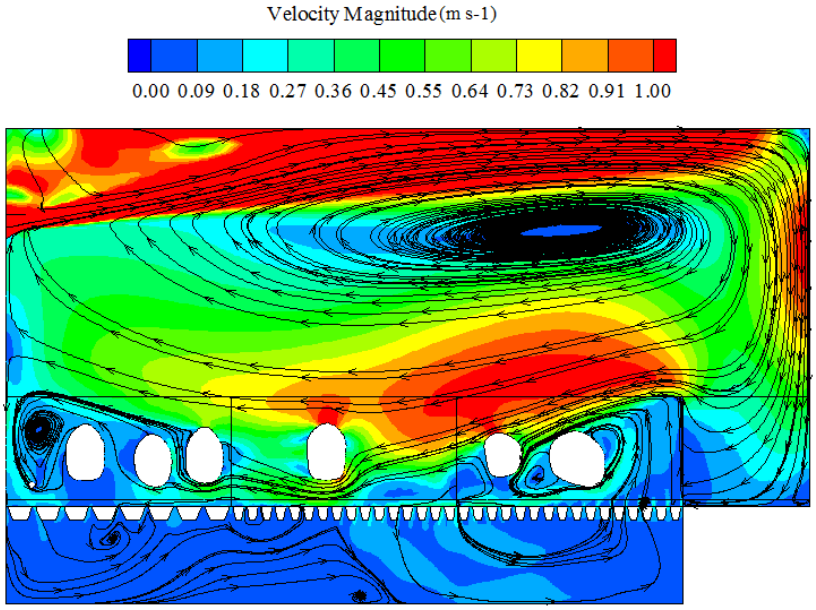

Figure 11 Contours of the velocity magnitude on the vertical plane in center of pen 2 in the case with pig model in real shape

5. Discussion

In the first parts of study, the experimental results were validated by the simulations. It should be noted that temperature was not studied as a parameter in this study. This was because the studied cases were under the configuration of mechanical ventilation, and the ventilation rate was relatively high, in which conditions the indoor air can be assumed to be fully mixed and with low temperature gradient.

Generally, good agreements were achieved, but still there were some deviations at different locations. In the aforementioned parts, it has been indicated that the turbulence models, the ratio on the interfaces, and the mesh types in the calculation domains might have impacts on the airflow pattern. All these simulation were conducted under a steady condition, while the real condition may not be strictly steady, the ventilation rate has fluctuations and vortexes can be generated in the wake of cylinder when the airflow passed. The transient RANS or LES calculation may provide better prediction on the airflow pattern, but the requirement of the computational power and time are more accordingly compared to the steady RANS method. Normally, the thermal comfort inside the livestock building depends on the temperature and airflow distribution in a long time span but not in temporary. In the validation experiment part, the measurement result was averaged from the data for at least 1 h. From this point, the usage of RANS which modelled the turbulence energy by time averaged method was a suitable way to describe the physical model in this study.

Besides the numerical errors, another reason for the discrepancy may come from the uncertainty of measurement, the uncertainty contain both the dimension of the geometry and the error of the sensors, but most of them were the uncertainty of the dimension measurement, take the inlet as an example, to simplify the modelling of geometry, only the main feature of the inlet was modelled, while some detailed geometry, like the tiny slots between the guiding plate and the frame were ignored. Those simplifications can lead to errors on the flow jet on the inlet.

In the last parts of the study, an example was provides in which the cylindrical models were replaced by pig models in real shape. Although the number of pig models was larger than the cylindrical models in the validation study, the physical models for these two cases were similar. It has been reported that the complex geometry make the airflow easier to be fully developed (Tian et al., 2015). Therefore, the example case can be validated by the case with simple cylindrical models. In the simulation, all the pig models were placed under a half stand and lying position, fully lying or standing postures were not modeled due to the complexity of geometry modelling. However, in real conditions, the pig may spend 90% time lying on the ground. The model in this study cannot be regarded as a strict description for the real case. From the Figure 11, it has been noticed that the airflow speed was very low in AOZ, due to the blocking from pigs. And the airflow passing the back of pig can be considered as main force for convective term of heat loss from pigs. Thus the impact from the pig postures can be very low, since the airflow inside the AOZ zone can be low due to the pig blocking. And therefore, the pigs can be arranged on a same height as a simplification to reduce the difficulty in geometry modelling. Overall, the purpose of the example here is providing the readers how the interface and unstructured mesh work to make the complex geometry mesh possible. The detailed model and meshing method depends on the research objectives.

6. Conclusions

This study evaluated the performance of five normally used two equations turbulence models, three cases using different ratios of interfaces boundary, and two mesh types on the AOZ sub-domain for predicting airflow distributions inside an experimental pig house. An example which showed how the interface and unstructured mesh work on modelling complex geometry contain pig models was provided. The conclusions are as followed:

The results showed that turbulence model had not strong effect on the main airflow pattern except the RNG k-ε model which deviated from other models in predicting the airflow distributions.

Within the three tested cases with varied ratios of the interface resolutions, no significant difference was found. And when the rations of the interface resolutions were higher, the number of mesh and computational time can be lower compared to the case when fully structured mesh was adopt. Considering the theory of data transfer on the interfaces, it is recommended having the ratio of interfaces on the interface close to 1.

The usage of unstructured mesh in the AOZ sub domain also provided acceptable results like the structured mesh. It is concluded that the non-conformal mesh can be applied in the study of animal building with complex geometry like animals.

Acknowledgements

Thanks to the support from research grant of Innovation Fund Denmark /Advanced Technology Foundation, New hot climate ventilation system for poultry and pigs (j.nr. 17-2013-3). And the thanks extend to China Scholarship Council (CSC) for the scholarship (201306350135) of Hao Li Ph.D. study in Denmark.

References

Anonymous, 2013a. ANSYS Fluent User's Guide(release 15.0). Ansys Inc., U.S.A.

Anonymous, 2013b. ANSYS FLUENT Theory Guide (release 15.0). ANSYS, Inc. , U.S.A.

Bartzanas, T., Boulard, T., Kittas, C., 2002. Numerical simulation of the airflow and temperature distribution in a tunnel greenhouse equipped with insect-proof screen in the openings. Comput Electron Agr 34, 207-221.

Bjerg, B., Svidt, K., Zhang, G., Morsing, S., Johnsen, J.O., 2002. Modeling of air inlets in CFD prediction of airflow in ventilated animal houses. Comput Electron Agr 34, 223-235.

Bjerg, B., Zhang, G., Kai, P., 2008. Porous media as boundary condition for air inlet, slatted floor and animal occupied zone in numerical simulation of airflow in a pig unit, Agricultural and biosystems engineering for a sustainable world. International Conference on Agricultural Engineering, Hersonissos, Crete, Greece, 23-25 June, 2008. European Society of Agricultural Engineers (AgEng), pp. OP-1520.

Brody, S., Comfort, E., Matthews, J.S., 1928. Further investigations on surface area with special reference to its significance in energy metabolism. Mo. Agr. Exp. Sta. Bull. 115.

Duan, R., Liu, W., Xu, L.Y., Huang, Y., Shen, X., Lin, C.H., Liu, J.J., Chen, Q.Y., Sasanapuri, B., 2015. Mesh Type and Number for the CFD Simulations of Air Distribution in an Aircraft Cabin. Numer Heat Tr B-Fund 67, 489-506.

Gebremedhin, K., Wu, B., 2005. Simulation of flow field of a ventilated and occupied animal space with different inlet and outlet conditions. J Therm Biol 30, 343-353.

Hefny, M.M., Ooka, R., 2009. CFD analysis of pollutant dispersion around buildings: Effect of cell geometry. Building and Environment 44, 1699-1706.

Huawei, S., Lingying, Z., Yuanhui, Z., 2007. Evaluating RNG κ-ϵ Models Using PIV Data for Airflow in Animal Buildings at Different Ventilation Rates. ASHRAE Transactions 113, 358-365.

Launder, B.E., Spalding, D.B., 1974. The numerical computation of turbulent flows. Computer Methods in Applied Mechanics and Engineering 3, 269-289.

Liu, W., Wen, J.Z., Lin, C.H., Liu, J.J., Long, Z.W., Chen, Q.Y., 2013. Evaluation of various categories of turbulence models for predicting air distribution in an airliner cabin. Building and Environment 65, 118-131.

Menter, F.R., 1994. Two-equation eddy-viscosity turbulence models for engineering applications. AIAA Journal 32, 1598-1605.

Norton, T., Grant, J., Fallon, R., Sun, D.W., 2010. Optimising the ventilation configuration of naturally ventilated livestock buildings for improved indoor environmental homogeneity. Building and Environment 45, 983-995.

Rong, L., Nielsen, P.V., Bjerg, B., Zhang, G., 2016. Summary of best guidelines and validation of CFD modeling in livestock buildings to ensure prediction quality. Comput Electron Agr 121, 180-190.

Seo, I.H., Lee, I.B., Moon, O.K., Hong, S.W., Hwang, H.S., Bitog, J.P., Kwon, K.S., Ye, Z.Y., Lee, J.W., 2012. Modelling of internal environmental conditions in a full-scale commercial pig house containing animals. Biosystems Engineering 111, 91-106.

Shen, X., Zhang, G.Q., Bjerg, B., 2012. Comparison of different methods for estimating ventilation rates through wind driven ventilated buildings. Energy and Buildings 54, 297-306.

Shih, T.-H., Liou, W.W., Shabbir, A., Yang, Z., Zhu, J., 1995. A new k-ϵ eddy viscosity model for high reynolds number turbulent flows. Comput. Fluids 24, 227-238.

Sorensen, D.N., Nielsen, P.V., 2003. Quality control of computational fluid dynamics in indoor environments. Indoor Air 13, 2-17.

Tian, E., He, Y.L., Tao, W.Q., 2015. Numerical Simulation of Finned Tube Bank Across a Staggered Circular-Pin-Finned Tube Bundle. Numer Heat Tr a-Appl 68, 737-760.
Wilcox, D.C., 1988. Reassessment of the scale-determining equation for advanced turbulence models. AIAA Journal 26, 1299-1310.
Wu, W.T., Zhang, G.Q., Bjerg, B., Nielsen, P.V., 2012. An assessment of a partial pit ventilation system to reduce emission under slatted floor - Part 2: Feasibility of CFD prediction using RANS turbulence models. Comput Electron Agr 83, 134-142.
Yakhot, V., Orszag, S.A., 1986. Renormalization-Group Analysis of Turbulence. Physical Review Letters 57, 1722-1724.
Zhang, Z., Zhai, Z.Q., Zhang, W., Chen, Q.Y., 2007. Evaluation of various turbulence models in predicting airflow and turbulence in enclosed environments by CFD: Part 2-comparison with experimental data from literature. Hvac&R Res 13, 871-886.